5-2011

Dispersion of the hyperpolarizability of the carbon tetrachloride molecule

Scott Wilde
University of Nevada, Las Vegas

DISPERSION OF THE SECOND HYPERPOLARIZABILITY OF THE CARBON TETRACHLORIDE MOLECULE

by

Scott Wilde

Bachelor of Science
University of Nevada, Las Vegas
2008

A thesis submitted in partial fulfillment of
the requirements for the

Master of Science in Physics
Department of Physics and Astronomy
College of Sciences

Graduate College
University of Nevada, Las Vegas
May 2011

UNIVERSITY OF NEVADA LAS VEGAS

THE GRADUATE COLLEGE

We recommend the thesis prepared under our supervision by

Scott Wilde

entitled

Dispersion of the Hyperpolarizability of the Carbon Tetrachloride Molecule

be accepted in partial fulfillment of the requirements for the degree of

Masters of Science in Physics
Department of Physics and Astronomy

David P. Shelton, Committee Chair

Victor H. S. Kwong, Committee Member

Stephen Lepp, Committee Member

Chulsung Bae, Graduate Faculty Representative

Ronald Smith, Ph. D., Vice President for Research and Graduate Studies
and Dean of the Graduate College

May 2011

ABSTRACT

Dispersion of the Second Hyperpolarizability of the Carbon Tetrachloride Molecule

by

Scott Wilde

Dr. David Shelton, Examination Committee Chair
Professor of Physics
University of Nevada, Las Vegas

The second hyperpolarizability of a molecule is the microscopic version of the third order susceptibility. Direct measurements of the ratio of the second hyperpolarizability of carbon tetrachloride to diatomic nitrogen are made possible through electric field induced second harmonic generation. Whenever the dispersion of the second hyperpolarizability is not negligible, there should be deviations from Kleinman symmetry. Previous experimental data for second hyperpolarizability of this molecule have only been at two frequencies and theory predicts the zero frequency value. In order to provide for a better extrapolation to zero frequency, additional gas phase measurements of this ratio at optical frequencies are presented and discussed.

TABLE OF CONTENTS

LIST OF TABLES

LIST OF FIGURES

CHAPTER 1

INTRODUCTION

A molecule in external fields will respond according to the strength of the applied fields. The subject of linear optics is the case where the material response is characterized by a linear coefficient multiplied by the applied field. For low amplitude electric fields the response is an induced electric dipole by the molecule that is linear in the field. The subject of nonlinear optics is concerned with the case of a nonlinear response to external fields. In the dipole approximation, the molecular response to external fields is modeled by the induced dipole. By Taylor expanding the polarization equation in powers of the electric field, the calculated response to strong fields will become nonlinear in terms of hyperpolarizabilities. In terms of static fields the dipole per molecule can be written as:

$$\mu = \mu^{(0)} + \alpha \mathrm{E}_0 + \frac{\beta}{2} \mathrm{E}_0^2 + \frac{\gamma}{6} \mathrm{E}_0^3 + \ldots \quad (1)$$

The terms that vary as the square of the field and the cube of the field are referred to as the first and second hyperpolarizabilities respectively. The first constant term in the expansion is referred to as the intrinsic dipole moment and it is nonzero for dipolar molecules. The vector nature of the polarization and the applied field(s) require that the polarization, α, be a second rank tensor, β a third rank tensor, γ a fourth rank tensor and so on. The field(s) in equation (1) has been represented as scalar(s) but in general the field(s) is vector quantities and can be oscillating with non-zero frequencies. As in most systems, symmetry can reduce the number of independent elements of tensors describing physical processes. Kleinman symmetry is a condition that is always valid at zero frequency, but for non-zero, and especially optical frequencies, deviations from

Kleinman symmetry become more apparent as frequency increases and approaches the threshold for absorption. In general, Kleinman symmetry is not valid where dispersion of the hyperpolarizability is not negligible. [1]

Sum frequency generation is the process where two or more photons are converted into one photon with a frequency equal to the sum of the frequencies of the incident photons. When the process takes two identical wavelengths and the resulting sum photon has half the wavelength it is called second harmonic generation (SHG). If the process occurs along a focused beam of photons, generated photons will begin to be out of phase with photons that are generated further along the beam path. It is possible to "match" the phase of generated photons from multiple sites by coherent addition. Phase matching is difficult to achieve in an isotropic medium such as a gas, but it can be done by introducing a periodic phase shift in one or more of the applied electric fields. A static and an optical field can be used to induce SHG from the third order response of the molecule, hence electric field *induced* second harmonic generation. If the direction of the static field is reversed periodically, then phase matching of the static field and the second harmonic can be found directly by scanning the density and measuring the second harmonic signal.

This work involves the measurement of the nonlinear properties of carbon tetrachloride (CCl_4) by using the technique of Electric Field Induced Second Harmonic Generation (EFISHG) for gas phase molecules. Resonant absorption is the process that makes both the deviations from Kleinman symmetry interesting and also the process that makes measurements difficult.

An additional complication comes from the CCl_4 low vapor pressure, and samples of high densities would require heating of the sample. By taking advantage of the experimentally measured hyperpolarizability for diatomic nitrogen (N_2) as a ratio to helium (He), for which an exact calculation can be done and has been done by Bishop and Pipin, the experiment can be done using mixtures as samples. [2, 3]

CHAPTER 2

THEORY

The following formulations are based on the work by Ward and New and also the work of Shelton and Buckingham. [4, 5] The static electric field in the y direction as a function of position along z, the axis of the fundamental beam propagation, can be defined as a periodic function.

$$\mathrm{E_y(z) = E_0 \cos(Kz)} \tag{2}$$

where $K=2\pi N/L$, where N is the number of periods, or pairs, L is the total length of the electrode array, and $\mathrm{E_0}$ is the static field amplitude. The phase mismatch between the fundamental, E_ω, and the second harmonic, $\mathrm{E}_{2\omega}$, is related to the difference of the index of refraction.

$$\Delta k = 2k_\omega - k_{2\omega} = \frac{4\pi}{\lambda_\omega}\left(n_\omega - n_{2\omega}\right) = \frac{-2\pi}{\lambda_\omega \varepsilon_0}\left(\alpha_{2\omega} - \alpha_\omega\right)\rho + \left(\text{terms in } \rho^2\right) \tag{3}$$

The phase is matched when $\Delta k = \pi / l_c$, where l_c is the coherence length of the gas. Therefore if the phase matching condition is satisfied, the second harmonic generated between each electrode pair will constructively interfere. Note that λ_ω is the wavelength of the fundamental in vacuum, n_ω is the index of refraction for frequency ω, and ρ is the density of the gas.

The optical field is defined as a Gaussian beam polarized parallel to the static field direction that is focused to a spot size defined by the confocal parameter z_0.

$$z_0 = \pi R_0^{\,2} n_\omega / \lambda_\omega \tag{4}$$

$$\left(R / R_0\right) = \sqrt{1 + \left(z / z_0\right)^2} \tag{5}$$

where R_0 is the radius of beam at the beam waist and R is the beam radius at a point z away from the beam radius. The maximum size, or diameter, of the beam that passes through the electrodes is therefore limited by diffraction. Diffraction sets an upper limit on how far apart and how many electrode pairs that the fundamental and second harmonic beams can pass through unobstructed. The case of a large number of repeats and a short distance between electrodes is preferred, but the optical field must pass through from outside the medium.

If the optical field is focused to the center of the electrode array, then the power generated at frequency 2ω can be written in terms of the power $P_{(\omega)}$ of the fundamental.

$$P^{(2\omega)} = \frac{\omega^3}{z_0 \pi c n_{2\omega}^2} \left(\frac{\mu_0}{\varepsilon_0} \right)^{\frac{3}{2}} \left(\chi^{(3)} \right)^2 \left(P^{(\omega)} \right)^2 {E_0}^2 \left(\int_{-L}^{L} dz \frac{\cos(Kz) \cos\left[\Delta k z - \arctan\left(z / z_0 \right) \right]}{\left[1 + \left(z / z_0 \right)^2 \right]^{\frac{1}{2}}} \right)^2 \qquad (6)$$

where the third order susceptibility, $\chi^{(3)}$, is defined in terms of macroscopic second hyperpolarizability, Γ. The macroscopic hyperpolarizability is related to the spatially averaged microscopic hyperpolarizability, γ, and, $\beta_{\|}$, which is the parallel component of β to the dipole moment.

$$\chi^{(3)} = \frac{1}{4} \mathscr{L}(0) \mathscr{L}^2(\omega) \mathscr{L}(2\omega) \Gamma \rho \qquad (7)$$

$$\Gamma = \langle \gamma \rangle + \frac{\mu^{(0)} \beta_{\|}}{3 k_B T} \qquad (8)$$

where $\mathscr{L}(\omega)$ is the Lorentz local field factor at frequency ω, defined as $\mathscr{L}(\omega) = \left(n_\omega^2 + 2 \right)/3$, and ρ is the number density of the gas molecules. The second term in equation (8) is an orientational average, and since the intrinsic dipole moment of CCl_4 is

zero, $\Gamma = \langle\gamma\rangle$, which simplifies the expression for the third order susceptibility in equation (7).

At phase match, the power of the second harmonic is peaked around $|\Delta k| = K$, and the height of the peak is proportional to N^2, with a width of $1/N$, because of the density dependence of $\chi^{(3)}$ and Δk. The peak power of the second harmonic beam is found by evaluating the integral in equation (6), which yields: [5]

$$P_{\text{peak}}^{(2\omega)} = \frac{\omega^3}{z_0 \pi c n_{2\omega}^2}\left(\frac{\mu_0}{\varepsilon_0}\right)^{\frac{3}{2}}\left(\chi^{(3)}\right)^2\left(P^{(\omega)}\right)^2 {E_0}^2 L\left[(z_0/L)\arctan^2(L/z_0)C(L/z_0)\right] \qquad (9)$$

where $C(L/z_0)$ is a slowly varying function near unity that depends on the focusing, z_0 and the length, L, of the electrode array. From here it is plain to see that the ratio of hyperpolarizabilities is easier to measure, provided a reference gas is available, instead of a direct measurement. The ratio of the power of the second harmonic for both CCl_4 and N_2, in the low density approximation, as long as all other experimental parameters stay the same, is written as:

$$\frac{P_{\text{peak}\ CCl_4}^{(2\omega)}}{P_{\text{peak}\ N_2}^{(2\omega)}} = \frac{S_{CCl_4}}{S_{N_2}} = \left(\frac{\gamma_{CCl_4}}{\gamma_{N_2}}\right)^2\left(\frac{\rho_{CCl_4}}{\rho_{N_2}}\right)^2 \qquad (10)$$

where S_{CCl_4} is the peak count rate for CCl_4. Since it would be proportional to the power by the same factor as the S_{N_2}, it can be shown that the ratio of peak second harmonic power for the pure gases is identically equal to the ratio of peak count rates from equation (9). For mixtures of low density, the ratio of phase matched power for a mixture of CCl_4 and N_2 can be written as:

$$\frac{\mathrm{P}_{\mathrm{mix}}^{(2\omega)}}{\mathrm{P}_{\mathrm{N}_2}^{(2\omega)}} = \frac{F \cdot S_{\mathrm{mix}}}{S_{N_2}} = \left[\frac{\gamma_{\mathrm{CCl}_4} x_{\mathrm{CCl}_4} \rho_{\mathrm{mix}} + \gamma_{\mathrm{N}_2} x_{\mathrm{N}_2} \rho_{\mathrm{mix}}}{\gamma_{\mathrm{N}_2} \rho_{\mathrm{N}_2}} \right]^2 \tag{11}$$

where x_{CCl_4} is the molar fraction of the carbon tetrachloride, and $x_{\mathrm{N}_2} = 1 - x_{\mathrm{CCl}_4}$, so the ratio of hyperpolarizabilities can be solved to be:

$$\frac{\gamma_{\mathrm{CCl}_4}}{\gamma_{\mathrm{N}_2}} = \frac{1}{x_{\mathrm{CCl}_4}} \left[\left(\frac{F \cdot S_{\mathrm{mix}}}{S_{\mathrm{N}_2}} \right)^{\frac{1}{2}} \frac{\rho_{\mathrm{N}_2}}{\rho_{\mathrm{mix}}} - 1 \right] + 1 \tag{12}$$

where *F* is the correction to the signal due to attenuation of the second harmonic by the sample, which is the ratio of the unabsorbed signal to the absorbed signal, calculation of this factor will be discussed later. Frequency doubled optical fields will start to approach the absorption band of the molecule and a correction must be calculated for the attenuation of the second harmonic to get the signal as if attenuation were not present. This can be done by calculating the ratio of the square of the amplitudes in the equation for the power of the second harmonic with an attenuation factor. The attenuation of the amplitude from one electrode pair, a site of generated second harmonic, is calculated with respect to the attenuation through the entire length of the cell. An attenuation coefficient in terms of the density of the gas in the cell can be used as an attenuation coefficient in a Beer-Lambert Law calculation for the length of the cell that the light passes through before exiting the attenuating medium.

$$t^2 = I / I_0 = e^{-2\alpha L} = e^{-a\rho} \tag{13}$$

$$\alpha = a\rho / 2L \tag{14}$$

where *a* is the attenuation in terms of the density of the gas and α is the attenuation coefficient that follows the Beer-Lambert law. The amplitude from one electrode site can

be approximated by using equation (6) and the attenuation due to the path through the rest of the sample in the cell. To find the amplitude of the combined second harmonic generated at sites along the electrode array one can calculate the sum of the amplitudes generated across the electrode array. [7]

$$I(\Delta k,\alpha)=\frac{\Delta k}{K}\frac{1}{2N}\sum_{n=-N}^{N-1}\left[\frac{\exp[-\alpha(x_c-x')/K]}{(1+u^2)^{\frac{1}{2}}}\right]\left[(1-\Delta k/K)\cos\varphi+\frac{(\cos\varphi+u\sin\varphi)}{x_0(1+u^2)}\right] \quad (15)$$

$$\varphi=\frac{K+\Delta k}{K}(x'-x_w)-\arctan u \quad (16)$$

$$u=(x'-x_w)/x_0 \quad (17)$$

$$x'=\left(n+\frac{1}{2}\right)\pi \quad (18)$$

The *x* parameters are the normalized parameters of the beam and cell, x_c is the position of the center of the array with respect to the output window multiplied by the period of the array, so that $x_c = Kz_c$, and so on for the other parameters. The factor by which the signal is attenuated is just the square of this amplitude divided by the square of the amplitude with no attenuation. The *F* factor in equation (12) is the square of the amplitude with no attenuation divided by the amplitude with attenuation squared.

$$F=\left[I(\Delta k,\alpha=0)_{\text{peak}}\Big/I(\Delta k,\alpha)_{\text{peak}}\right]^2 \quad (19)$$

where $I(\Delta k,\alpha=0)_{\text{peak}}$ is the calculated peak amplitude from equation (15) with α = 0, and $I(\Delta k,\alpha)_{\text{peak}}$ is the attenuated signal. The measured signal, S_{mix} in equations (11) and 12, of a sample that attenuates the generated signal along the beam path will be

attenuated by 1/*F* and the second harmonic generated signal will be *F* times the measured signal.

In birefringent crystals, the phase match condition can be met for optical fields by changing the orientation of the crystal axes to the optical field. By using a quartz wave plate in the beam to convert the fundamental into double the frequency, one can measure the attenuation of the through the length of the cell as a function of density. Therefore the right hand side of equation (13) can be measured by slowly filling the cell with CCl_4 and measuring the attenuation of the signal from the quartz plate as a function of fill pressure, which can be converted to a function of the length of the gas cell the second harmonic travels through before it exits the cell. This is used to determine the attenuation correction.

Kleinman symmetry imposes the condition that the susceptibility is invariant under permutation of spatial indices, such that if the frequency components were all zero you would have perfect permutation symmetry and thus Kleinman symmetry is everywhere valid in the zero frequency limit. [3] In the case for EFISHG, the third order susceptibility has four indices, and four frequency arguments, as shown in the full macroscopic polarization, *P*, in equation (20), excluding lower order terms.

$$P_i(2\omega) = \tfrac{3}{2}\chi_{ijkl}(-2\omega;\omega,\omega,0)\mathrm{E}_j(\omega)\mathrm{E}_k(\omega)\mathrm{E}_l(0) \qquad (20)$$

The electric field in the j-th direction that is oscillating with a frequency ω is denoted by the $\mathrm{E}_j(\omega)$, where the polarization in the i-th direction oscillating at a frequency of 2ω is $P_i(2\omega)$. For an isotropic gas, the susceptibility tensor should also be isotropic, which means that there will be at most two independent elements which can be written as a sum.

$$\chi_{zzzz}(-2\omega;\omega,\omega,0) = \chi_{zxxz}(-2\omega;\omega,\omega,0) + 2\chi_{zxzx}(-2\omega;\omega,\omega,0) \qquad (21)$$

where $\chi_{zxzx}(-2\omega;\omega,\omega,0) = \chi_{zzxx}(-2\omega;\omega,\omega,0)$ because permuting the indices of the optical fields of the same frequency should be indistinguishable. At zero frequency, if the frequency components are interchanged simultaneously with the spatial components and the components of the sum are left unchanged then the independent elements must be equal, in other words $\chi_{zzzz}(0;0,0,0) = 3\chi_{zxxz}(0;0,0,0)$, and the ratio of the susceptibilities should yield R(ω=0) = 3 as shown in equation (24). This type of symmetry is referred to as *intrinsic* permutation symmetry.

$$\mathrm{R}(\omega) = \chi_{zzzz}(-2\omega;\omega,\omega,0) / \chi_{zxxz}(-2\omega;\omega,\omega,0) \tag{22}$$

Measurements of this ratio for different frequencies will be in effect measuring deviations from Kleinman symmetry. Using the dipole approximation further, the displacement of the electron cloud for the molecule can be modeled as a driven electron on a spring oscillator with complex frequency components. Taking the real part and expanding that in terms of frequency will result in an expansion in even powers of frequency. The same can be done for the second hyperpolarizability,

$$\gamma(-2\omega;\omega,\omega,0) = \gamma(0;0,0,0)\left(1 + a_1\omega^2 + a_2\omega^4 + \ldots\right) \tag{23}$$

Several theoretical techniques are used to calculate the zero frequency value, and the burden on the experiment is to provide an extrapolation to zero frequency. As the frequency increases to the optical, oscillations will occur so quickly that the nuclei in the molecule will be near stationary and the only contribution to the hyperpolarizability will be the electronic part. The EFISHG experiment using vapor phase molecules and optical frequencies is essentially probing only the electronic part of the hyperpolarizability. An extrapolation to zero frequency using optical frequencies will then result in a reliable estimate for the zero frequency hyperpolarizability.

The Kleinman symmetry ratio can also be modeled using a power series expansion in even powers of the frequency because of the relationship it has with the hyperpolarizability.

$$\mathrm{R}(\omega) = 3\left(1 + b_1\omega^2 + b_2\omega^4 + \ldots\right) \tag{24}$$

As the strength of the dependence of the hyperpolarizability on frequency becomes more apparent, there should also be deviations from Kleinman symmetry. The measured signal from a pure gas in an optical field polarized parallel to the static field would be proportional to the square of $\chi_{zzzz}(-2\omega;\omega,\omega,0)$, and the measured signal from a pure gas in an optical field polarized perpendicular to the static field is proportional to the square of $\chi_{zxxz}(-2\omega;\omega,\omega,0)$, as shown in equation (25).

$$\mathrm{R}_{\mathrm{exp}} = \left(\frac{S_{\parallel}}{S_{\perp}}\right)^{\frac{1}{2}} = \chi_{zzzz} / \chi_{zxxz} = \gamma_{\parallel} \Big/ \gamma_{\perp} = \langle\gamma\rangle_{zzzz} \Big/ \langle\gamma\rangle_{zxxz} \tag{25}$$

where the brackets around γ indicate an orientation average. The measured hyperpolarizability ratio of CCl_4 and N_2 from EFISHG will be $\gamma_{\parallel,\,\mathrm{CCl_4}} / \gamma_{\parallel,\,\mathrm{N_2}}$. For a low density mixture of two gases, the expression for the measured ratio can be written as equation (26), in terms of the mixture density as,

$$R_{\mathrm{mix}} = \left[S_{\mathrm{mix},\parallel} \Big/ S_{\mathrm{mix},\perp} \right]^{\frac{1}{2}} = \frac{\gamma_{\parallel,\,\mathrm{CCl_4}} x_{\mathrm{CCl_4}} \rho_{\mathrm{mix}} + \gamma_{\parallel,\,\mathrm{N_2}} x_{\mathrm{N_2}} \rho_{\mathrm{mix}}}{\gamma_{\perp,\,\mathrm{CCl_4}} x_{\mathrm{CCl_4}} \rho_{\mathrm{mix}} + \gamma_{\perp,\,\mathrm{N_2}} x_{\mathrm{N_2}} \rho_{\mathrm{mix}}} \tag{26}$$

and this equation can be manipulated by using the ratio of hyperpolarizabilities for the two gases in the mixture,

$$\frac{1}{\mathrm{R}_{\mathrm{CCl_4}}} = \frac{1}{\mathrm{R}_{\mathrm{mix}}} + \left(\frac{1}{\mathrm{R}_{\mathrm{mix}}} - \frac{1}{\mathrm{R}_{\mathrm{N_2}}}\right) \frac{\gamma_{\mathrm{CCl_4}}}{\gamma_{\mathrm{N_2}}} \frac{x_{\mathrm{CCl_4}}}{\left(1\text{-}x_{\mathrm{CCl_4}}\right)} \tag{27}$$

where R_{CCl_4} is the ratio for pure carbon tetrachloride, R_{N_2} is the ratio for pure nitrogen, and R_{mix} is the ratio for the mixture. The molar fraction of nitrogen, x_{N_2}, can be written in terms of the molar fraction of carbon tetrachloride, x_{CCl_4}, which is just $x_{N_2} = (1-x_{CCl_4})$, note that this is true for binary mixtures.

CHAPTER 3

EXPERIMENTAL METHODS

The optical fields available and used to measure the ratio of hyperpolarizabilities were two laser lines from an argon ion laser, λ = 488.0nm and λ = 514.5nm, which produced second harmonic of wavelength 244.0nm and 257.3nm, respectively. The fundamental beam is weakly focused to a confocal length of 48.85cm and 45.92cm through the electrode array. Note this is the confocal parameter for the unfilled gas cell. A diagram of the experimental setup is shown in figure 1; a representative line is drawn to show the path of the beam through the apparatus. The beam is weakly focused through the cell and the beam profile was measured by using a Thor Labs beam profiler for both wavelengths prior to installation of the gas cell. The diameter of the beam as a function of position was fit to a hyperbola to find the position of the beam waist with respect to the center of the electrode array. Periodically throughout the experiment the beam divergence was measured downstream from the cell to verify the beam profile had not changed.

The windows of the cell containing the electrodes and the gas were made of fused silica to pass the ultraviolet. Since fused silica is susceptible to stress induced birefringence, it was important to minimize translational force gradients in the window. The windows were sandwiched between two polytetraflouroethylene (PTFE, Teflon) O-rings so that the window would seal against the outer O-ring and the inner O-ring served as a spring feedback when installing the window in the cell.

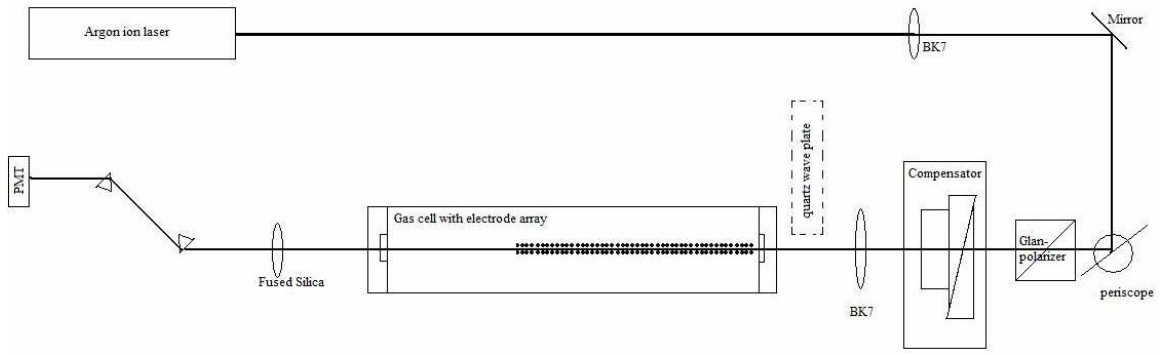

Figure 1: Diagram of experimental setup.

The gas was introduced to the cell by way of a manifold of shut-off valves and copper tubing and the pressures were measured by a MKS Instruments Baratron Transducer, the output of which was recorded with an Analog to Digital Converter (ADC) sensitive to micro-volt ranges. The cell is pumped down to a few mTorr through a liquid nitrogen cold-trap by a roughing pump. The cell was filled either with pure N_2 or with a mixture. Prior to filling, the cell was flushed with N_2 at 1 atmosphere and the CCl_4 had been put through several freeze, pump, and thaw cycles to pump away dissolved atmospheric gas.

The electrode array used in the experiment had 80 repeats, or 160 total cylindrical electrodes. Spacing between the surfaces of the electrodes was 0.71mm, spacing between electrode centers was 1.27mm and the total length of the electrode array was 20.3cm. Other electrode arrays with varying spacing had been investigated to see if the signal from pure CCl_4 was high enough to perform the experiment on a pure gas sample of CCl_4. Count rates for the pure gas were low enough to need several hours for one measurement. Since the signal from a mixture using the fine array mentioned previously was found to be several orders of magnitude larger than the best that could be found from other available electrode arrays and a pure sample of CCl_4, the choice was made to use

mixtures of N_2 and CCl_4. Attached to the electrode array is a plate that makes contact with a high voltage power supply through the gas cell wall. The only available feed through ports for the high voltage power supply was on either end of the cell, and the electrode array was positioned on the front end of the cell. This geometry is a result of the beam waist position from the lenses and the space needed to introduce the quartz plate in front of the cell for both alignment and attenuation measurements. The preferred orientation would have been to focus the fundamental beam even less so that the BK7 lens could be further away from the cell and the array on the far end of the cell. This would have minimized the attenuation from the gas in the cell because the second harmonic would have had to travel less distance through the sample before exiting the cell. The second harmonic travels collinearly with the fundamental beam, and so it is separated from the fundamental beam by using a double prism spectrometer.

A set of mirror mounts were used to mount mirrors in a periscope configuration, the first mirror would reflect the beam upwards and the second would reflect back down to the horizontal and turn the beam to pass through the cell. As a consequence of this beam steering, the polarization of the beam was also rotated by the reflections to a horizontal polarization state before entering the prism polarizer. By using a crossed polarizer, the angle of extinction was measured to be 89.9 ± 0.1 degrees in reference to the horizontal.

Initially the photomultiplier (PMT) used was a Hamamatsu R1527P, reflection type photocathode, but during the experiment it became apparent that a different PMT was needed. A wire mesh obstruction, which is meant to focus the photoelectrons to the first dynode, also obstructed the signal beam. The beam spot size at the window to the photodetector was about the size of the wires in the mesh, there was a strong systematic

error introduced in the Kleinman symmetry measurements from beam steering from the change in the polarization. The part of the beam would overlap over the wire mesh for one polarization and a different overlap would be for another polarization of the fundamental. Since the compensator could be adjusted for up to three wavelengths path difference, it would be possible to measure the effect of beam steering and find a correction. An alternative was to use a different PMT, yet all that was available was one that had been used in several experiments prior to the first. The advantage was it was without the mesh, because it had a transmission photocathode, but the price was lower signal. Fortunately the signal was high enough that it would take approximately the same amount of time to obtain large enough statistics that it would take measure the systematic error that the reflection photocathode PMT introduced. All the measurements for Kleinman symmetry deviations required the use of this PMT in order to achieve a precision of <0.1% but some of the measurements for the second hyperpolarizability were done using the first PMT since the polarization was unchanged during those measurements.

The input polarization state of the optical field is prepared by using a Glan-laser prism polarizer in order to have a well defined horizontal polarization. The polarization is then controlled by using a Special Optics Soleil-Babinet compensator. The different polarization settings of the compensator would still steer the beam and even though the mesh-less PMT was used, sometimes there would still be a detectable difference from one polarization to another. One method to reduce this effect was to average across a vertical polarization state defined by rotating the horizontal through a positive rotation and then through a negative rotation in reference to the fundamental beam propagation

direction. The first analysis of a data set was a comparison between the vertical polarizations. If both did not agree within the statistical error then the measurements from that data set were abandoned.

The argon ion laser has an intense plasma glow that overlaps the ultraviolet that is detectable even through the spectrometer. To mitigate this and also to address the second harmonic light generated by the polarization control components, the lens just before the input window of the gas cell is made out of borosilicate (BK7) glass which strongly absorbs in the ultraviolet. A further measure to prevent coherent interference with second harmonic light generated outside the cell is to reverse the direction of the static field and take the average of measurements of one direction and the other. The interference term from a 180 degrees phase shift will exactly cancel out in an average. This is necessary because a weak source of second harmonic light generated along the beam path will interfere with the light generated inside the cell and will change the measured signal. Large effects were seen using the quartz plate in both upstream and downstream, and some cases were observed to nearly cancel out a phase matched signal. For normal experimental conditions, the signals from both directions of the static field were in agreement.

To prevent temporal shifts in the apparatus to bias the data, measurements were taken in ABA triplets, and the average taken over each triplet. For the Kleinman symmetry measurements, each measured value would be taken with both polarities of the static field,

$$(\leftrightarrow,+)(\leftrightarrow,-)(\uparrow,-)(\uparrow,+)(\leftrightarrow,+)(\leftrightarrow,-)(\downarrow,-)(\downarrow,+)(\leftrightarrow,+)(\leftrightarrow,-)... \qquad (29)$$

where $(\leftrightarrow,+)(\leftrightarrow,-)$ is an average of the two sequential horizontal measurements, $\leftrightarrow$ indicates the polarization is along the horizontal, the + means positive polarity and – means negative polarity of the static field. The parentheses represent one separate measurement, so the horizontal measurement is a measurement of the positive polarity across the electrode array and the negative polarity averaged together. The polarization was rotated in two different directions, and so those measurements are indicated as $\uparrow$ for a positive rotation and $\downarrow$ for negative rotation, and both are vertically polarized.

For the hyperpolarizability data, the measured values that are extracted are the peak density and count rate. Both are found by filling the cell to well above peak density, then slowly leaking the sample gas and measuring pressure, temperature, and count rate as the pressure went over the peak to the other side. Then the peak pressure and count rate can be found by fitting a parabola, $s = b(x-c)^2 + S$, where S is the peak signal count rate, s is the signal count rate, x is the pressure, and c is the peak pressure. An example of such a measurement is found in figure 2, where the solid line is the weighted parabolic fit. The range of points used in the fit is the top half of the peak. The signal in figure 2 is from a N_2 sample.

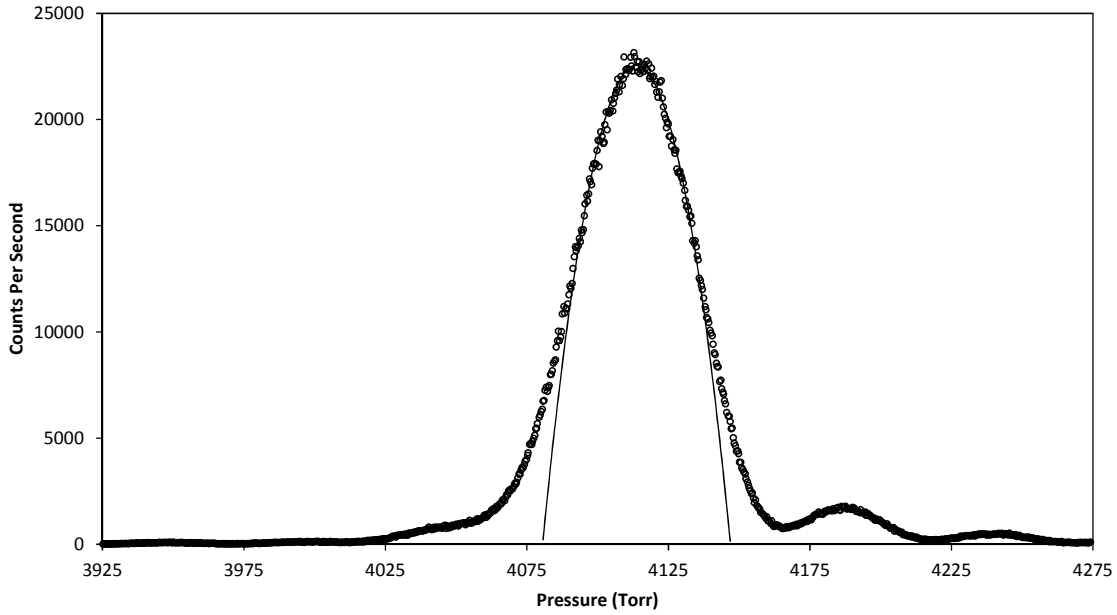

Figure 2: Example measured signal (open circles) and parabolic fit (solid line)

The temperature was measured by a type K thermocouple in contact with the gas at roughly 295K. Peak density is determined by using the temperature and the peak pressure by application of the virial equation of state. The gas mixtures were prepared by first filling with CCl_4 while simultaneously measuring the attenuation as a function of fill pressure. Then the cell was filled with N_2 until the pressure of the mixture was just above the expected peak pressure and the cell was allowed to come to equilibrium. Minimal fluctuations of the temperature inside the cell after filling were what determined the equilibrium condition. The molar fractions are determined by taking the ratio of the densities calculated from the fill pressures:

$$x_{CCl_4} = \rho_{CCl_4} \Big/ \rho_{mix} \tag{27}$$

$$x_{N_2} = 1 - x_{CCl_4} \tag{28}$$

The virial coefficient for a mixture of N_2 and CCl_4 is determined by using the virial equation of state for a mixture as shown below

$$B_{(T)} = B_{N_2(T)} x_{N_2}^2 + 2B_{mix(T)} x_{N_2} x_{CCl_4} + B_{CCl_4(T)} x_{CCl_4}^2 \quad (29)$$

$$\rho = 1 / (RT/P + B_{(T)}) \quad (30)$$

where $B_{N_2(T)}$ is the virial coefficient for pure N_2, $B_{CCl_4(T)}$ is for pure CCl_4, $B_{mix(T)}$ is the interaction virial coefficient or cross virial coefficient at temperature T, R is the gas constant, and P is the pressure of the gas. [8]

CHAPTER 4

MEASUREMENTS AND RESULTS

An example of an attenuation measurement is shown in figure 3, the case shown is for 488.0nm, or 244.0nm.

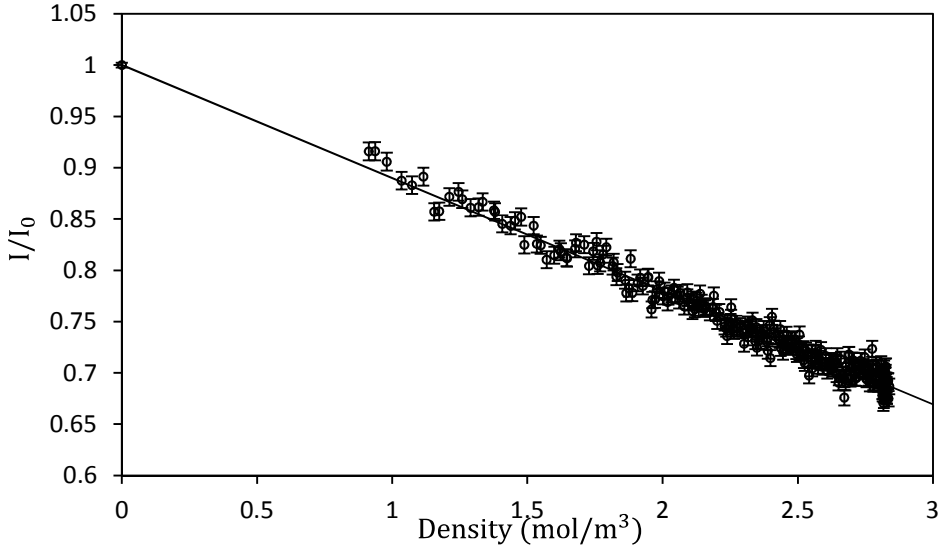

Figure 3: Attenuation of the frequency doubled 488.0nm signal from SHG in quartz

The solid line is a weighted linear fit to the data, $I/I_0 = 1 + a\rho$, where a is the attenuation coefficient that depends on density, this value is used to determine the Beer-Lambert law attenuation coefficient and I/I_0 is the ratio of the signal to the signal with CCl_4 in the cell. The length of the gas the beam travels through was measured window to window to be 50.43 ± 0.08 cm. The average attenuation coefficient measured by this method for 244nm is a = -0.1082 ± 0.0018 m^3/mol, and for 257nm a = -0.01562 ± 0.00040 m^3/mol. These values were used to calculate F in equation 19, the peak density for each mixture was used to calculate α and the signal for each mixture is corrected by

this factor in tables 1 and 2. The average cross section for 244nm is in agreement by a factor of two from an extrapolation of measurements in the ultraviolet of the cross section for CCl_4 from measurements by Carlon, *et. al*. Their measurements were from 185.0nm to 228.8nm and their measured cross section for 228.8nm is about two decades larger than what was measured for 244.0nm in this experiment. [9]

Table 1: Hyperpolarizability measurements for 488.0nm

Sample	S (cps)	F	S_{mix} (cps) $(= F \cdot S)$	Pressure (Torr)	Temp (K)	Peak Density (mol/m^3)	x_{CCl_4} (%)	$\gamma_{CCl_4} / \gamma_{N_2}$
N_2	23148.91			3443.21	295.15	187.23 ± 0.14		
$CCl_4 + N_2$	24131.39	1.218 ± 0.016	29392.75	2880.86	295.15	156.73 ± 0.12	1.750 ± 0.047	20.51 ± 0.73
N_2	23389.91			3437.21	295.15	186.91 ± 0.14		
$CCl_4 + N_2$	24546.71	1.220 ± 0.016	29937.46	2882.60	295.15	156.83 ± 0.12	1.761 ± 0.047	20.29 ± 0.73
N_2	23931.41			3432.79	295.15	186.67 ± 0.14		
$CCl_4 + N_2$	24718.31	1.222 ± 0.017	30194.95	2875.91	295.15	156.47 ± 0.12	1.780 ± 0.047	20.57 ± 0.73
N_2	23350.21			3432.75	295.15	186.66 ± 0.14		
N_2	2068.57			3431.88	293.95	185.40 ± 0.14		
$CCl_4 + N_2$	2098.51	1.230 ± 0.016	2582.124	2900.10	294.00	156.42 ± 0.12	1.734 ± 0.049	19.96 ± 0.74
N_2	2052.62			3442.82	294.05	185.93 ± 0.14		
$CCl_4 + N_2$	2093.51	1.222 ± 0.017	2557.690	2914.51	294.35	157.02 ± 0.12	1.775 ± 0.048	19.11 ± 0.71
N_2	2056.23			3447.75	294.35	186.01 ± 0.14		
N_2	2058.89			3441.94	294.35	185.69 ± 0.14		
$CCl_4 + N_2$	2089.1	1.220 ± 0.016	2548.771	2912.46	294.45	156.85 ± 0.12	1.764 ± 0.048	19.00 ± 0.71
N_2	2058.12			3443.41	294.35	185.77 ± 0.14		
N_2	2495.67			3408.12	294.75	185.55 ± 0.14		
$CCl_4 + N_2$	2562.32	1.231 ± 0.016	3154.858	2887.50	294.85	157.23 ± 0.12	1.731 ± 0.47	20.20 ± 0.73
N_2	2460.64			3414.85	294.95	185.80 ± 0.14		
N_2	2107.77			3424.96	295.65	185.90 ± 0.14		
$CCl_4 + N_2$	2179.77	1.225 ± 0.016	2670.717	2894.00	296.05	156.94 ± 0.12	1.689 ± 0.045	21.66 ± 0.76
N_2	2019.95			3436.34	295.95	186.33 ± 0.14		

After the peak densities, count rates, and signal attenuation are measured, the ratio of the hyperpolarizabilities can be determined by using equation (12) for the mixtures. The errors in peak pressure and peak count rates from the parameters of the parabolic fits such

as figure 2 were small, < 0.01%, that they were omitted from the table. Measurements for 488.0nm are found in table 1.

The following pertains to measurements done after the first measured value of the hyperpolarizability ratio for 514.5nm which appears as the first three rows of table 2. It was found that for the measurements of 514.5nm there was contamination of the cell with carbon tetrachloride during measurements of the pure nitrogen samples. Measurements that were intended to be for an uncontaminated sample were shifted towards a mixture measurement by left over sample between measurements. Previous work involving the same electrode array had measured the peak density as 222 mol/m^3 and this work has an average of 219 mol/m^3 for 514.5nm. [10] The peak density found by using the parabolic fits to the data are reported in table 2, but the peak density used in the hyperpolarizability ratio calculation for pure N_2 was 222 mol/m^3.

Table 2: Hyperpolarizability measurements for 514.5nm

Sample	S (cps)	F	S_{mix} (cps) (=$F \cdot S$)	Pressure (Torr)	Temp (K)	Peak Density (mol/m^3)	x_{CCl_4} (%)	$\gamma_{CCl4} / \gamma_{N_2}$
N_2	2054.48			4128.78	295.15	222.48 ± 0.15		
$CCl_4 + N_2$	2335.34	1.0279 ± 0.0028	2400.43	3569.84	295.15	192.20 ± 0.13	1.469 ± 0.038	17.91 ± 0.46
N_2	2078.68			4134.02	295.15	222.77 ± 0.15		
N_2	21526.0			4020.96	295.25	218.51 ± 0.15†		
$CCl_4 + N_2$	24530.3	1.0300 ± 0.0027	25265.9	3564.19	295.25	191.82 ± 0.13	1.417 ± 0.038	18.93 ± 0.50
N_2	21511.0			4045.10	295.25	217.86 ± 0.15†		
$CCl_4 + N_2$	25024.2	1.0289 ± 0.0027	25746.9	3597.22	295.25	191.62 ± 0.13	1.416 ± 0.038	19.72 ± 0.52
N_2	21683.0			4017.12	295.25	216.34 ± 0.15†		
N_2	21500.4			4053.54	295.35	218.32 ± 0.15†		
$CCl_4 + N_2$	24725.2	1.0292 ± 0.0027	25447.6	3564.61	295.25	191.82 ± 0.13	1.432 ± 0.038	19.12 ± 0.50
N_2	21477.9			4038.54	295.25	217.65 ± 0.15†		
N_2	22068.0			4077.83	295.00	220.06 ± 0.15†		
$CCl_4 + N_2$	24521.7	1.0614 ± 0.0028	26026.9	3565.39	295.00	192.05 ± 0.13	1.407 ± 0.038	19.06 ± 0.51
N_2	22157.5			4076.85	295.15	219.90 ± 0.15†		
$CCl_4 + N_2$	23802.1	1.0751 ± 0.0028	25590.1	3557.87	295.15	191.54 ± 0.13	1.423 ± 0.038	19.16 ± 0.51
N_2	21260.0			4078.60	295.05	219.75 ± 0.15†		
$CCl_4 + N_2$	22959.4	1.0707 ± 0.0025	24581.7	3553.92	295.15	191.33 ± 0.13	1.414 ± 0.038	19.80 ± 0.52
N_2	20047.9			4096.39	295.45	220.50 ± 0.15†		

†measured contaminated phase match density for N_2

A summary of the measured ratio of hyperpolarizabilities are found in the table 3 and plotted versus wavenumber in figure 4. Solid data points are from previous work, and the solid line is a weighed linear fit to the data. The point at zero frequency is the calculated zero frequency value, the size of the point is not intended to indicate error.

Table 3: Summary of measured hyperpolarizability ratios

Wavelength (nm)	$\gamma_{CCl4}/\gamma_{N_2}$	$\langle\gamma_{CCl4}/\gamma_{N_2}\rangle$
488.0	20.51 ± 0.73 20.29 ± 0.73 20.57 ± 0.73 19.96 ± 0.74 19.11 ± 0.71 19.00 ± 0.71 20.20 ± 0.73 21.66 ± 0.76	20.13 ± 0.26
514.5	17.91 ± 0.46 18.93 ± 0.49 19.72 ± 0.52 19.12 ± 0.50 19.06 ± 0.51 19.15 ± 0.51 19.80 ± 0.52	19.05 ± 0.19
694.3[a]		15.59 ± 0.19
1064[b]		12.82 ± 0.21
-		14.41[c]

[a] see reference [13], [b] see reference [11], [c] calculated zero frequency value, reference [16]

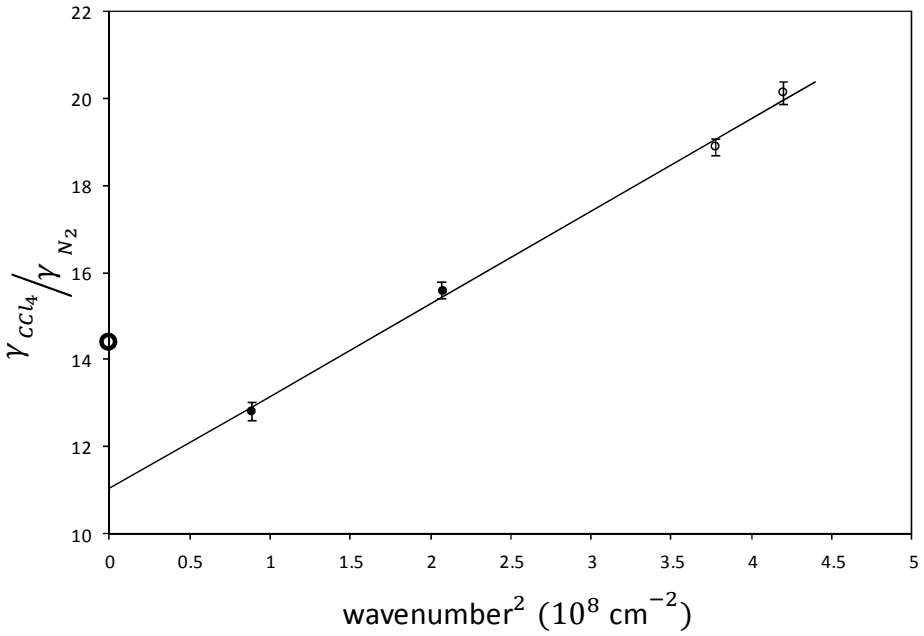

Figure 4: Measured hyperpolarizability ratios plotted versus wavenumber squared.

The value for the zero frequency value of the ratio is 10.99 ± 0.14, and the slope is 2.158 ± 0.035 cm^2 found from the weighted linear fit. The major contribution to the error in the hyperpolarizability ratio is from the molar fraction of the CCl_4 in the mixture. The error in the molar fraction for CCl_4 was estimated by the estimate of the error in the fill pressure and temperature. The fill pressure for CCl_4 for all samples was 52 Torr and the error was estimated by using the statistical spread in fill pressures measured at 1 second intervals by the ADC manometer combination. The error contribution from the molar fraction was 1-2% to the hyperpolarizability ratio. Following the molar fraction the next major contribution to the error in the hyperpolarizability ratio is from the error in the correction term from the attenuation, which was less than 0.3%, it was calculated by propagating the errors through the sum in equation (15). The main contribution to the error in the attenuation correction was from the error in the density dependent attenuation factor from the weighted linear least squares such as in figure 3.

As shown in equation (25), the ratio for Kleinman symmetry using mixtures requires the measured value of the ratio of hyperpolarizabilities and the ratio, R, for the pure nitrogen in order to calculate the R value for carbon tetrachloride. Measurements were made using pure nitrogen and are tabulated in table 4. The weighted means of the measurements are indicated in the second to last column and in the last column are measurements made by Mizrahi and Shelton. [12]

Table 4: Kleinman symmetry measurements of N_2

Wavelength (nm)	R_{N_2}	$\langle R_{N_2} \rangle$	R[a]
514.5	2.9453 ± 0.0022 2.9478 ± 0.0026 2.9475 ± 0.0024 2.9470 ± 0.0024 2.9500 ± 0.0026 2.9505 ± 0.0027 2.9434 ± 0.0030	2.947 ± 0.001	2.945 ± 0.003
488.0	2.9372 ± 0.0040 2.9368 ± 0.0025 2.9385 ± 0.0028 2.9363 ± 0.0030 2.9400 ± 0.0027 2.9409 ± 0.0022	2.939 ± 0.001	2.942 ± 0.004

[a] from reference [12]

After the mixture is prepared the triplet measurements would run about 10-20 triplets per mixture, for between 45-75 seconds for each measurement. The results from the measurements of several mixtures are tabulated in table 5 and each value corresponds to one mixture.

Table 5: Kleinman symmetry measurements for gas mixtures and calculated ratios for pure CCl_4

Wavelength (nm)	$R_{N_2+CCl_4}$	x_{CCl_4}	R_{CCl_4}	$\langle R_{CCl_4} \rangle$
514.5	2.9863 ± 0.0017	1.426 ± 0.043	3.137± 0.036	3.113 ± 0.016
	2.9838 ± 0.0018	1.390 ± 0.042	3.128 ± 0.036	
	2.9831 ± 0.0030	1.459 ± 0.044	3.117 ± 0.037	
	2.9781 ± 0.0017	1.374 ± 0.038	3.100 ± 0.037	
	2.9721 ± 0.0021	1.265 ± 0.038	3.078 ± 0.037	
488.0	3.0032 ± 0.0056	1.690 ± 0.051	3.206 ± 0.035	3.123 ± 0.018
	2.9799 ± 0.0045	1.719 ± 0.052	3.103 ± 0.037	
	2.9753 ± 0.0061	1.704 ± 0.051	3.084 ± 0.037	
	2.9777 ± 0.0048	1.753 ± 0.053	3.091 ± 0.037	
	2.9799 ± 0.0045	1.756 ± 0.053	3.100 ± 0.037	

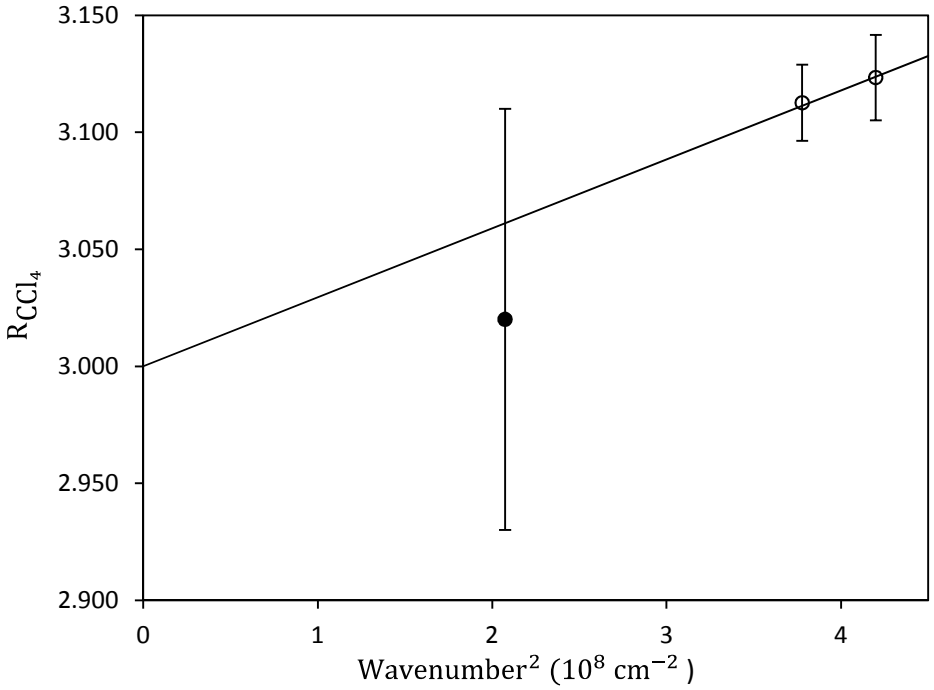

Figure 5: Deviations from Kleinman symmetry for CCl_4.

Following the same expansion of even powers in frequency and the results from the ratio of hyperpolarizabilities, it is expected that the measurements will fall on a straight line that intercepts 3 at zero frequency plotted against frequency squared or wavenumber squared as shown in figure 5. The solid point is a previous measurement done by Ward and Miller. [13]

The errors in the Kleinman symmetry ratios were calculated using estimated errors for the molar fraction of CCl_4, the statistical error in the mixture and pure nitrogen measurements, and the calculated error for the mean of the measured hyperpolarizability ratio.

Requirements were imposed on data points taken during Kleinman symmetry measurements that resulted in some triplets to not be used in the final result. If a triplet disagreed with the weighted mean by twice the statistical error it was not used in the final

result of the mixture. The number of omitted triplets under this criterion was less than one per mixture.

CHAPTER 5

CONCLUSION

The zero frequency value for $\gamma_{CCl4}/\gamma_{N_2}$ was found to be 11.04 ± 0.14. The zero frequency value is calculated as 14.41 by Ohta, et. al., as indicated by the open point in figure 4. [15, 16] It appears that a linear relationship between the hyperpolarizability of CCl_4 and wavenumber squared is adequate to describe the dispersion of the hyperpolarizability even in the optical range. Similarly for the deviations from Kleinman symmetry, even though they are large as compared to deviations for other molecules that have been measured. [12]

REFERENCES

[1] D. A. Kleinman, Phys. Rev. **126**, 1977 (1962)

[2] D. M. Bishop and J. Pipin, J. Chem. Phys. **91**, 3549 (1989)

[3] V. Mizrahi and D. P. Shelton, Phys. Rev. Lett., **55**, 696 (1985)

[4] J. F. Ward and G. H. C. New, Phys. Rev. 185, 57 (1969)

[5] D. P. Shelton and A. D. Buckingham, Phys. Rev. A **26**, 5 (1982)

[6] D. P. Shelton, J. Opt. Soc. Am. B **12**, 1880 (1985)

[7] D. P. Shelton, Chem. Phys. Lett., **121**, 69 (1985)

[8] J. H. Dymond and E. B. Smith, *The Virial Coefficients of Pure Gases and Mixtures* (Clarendon, Oxford, 1980).

[9] N. Rontu Carlon, D. K. Papanastasiou, E. L. Fleming, C. H. Jackman, P. A. Newman, and J. B. Burkholder, Atmos. Chem. Phys., **10**, 6137 (2010).

[10] E. A. Donley and D. P. Shelton, Chem. Phys. Lett., **215**, 156 (1993)

[11] P. Kaatz, E. A. Donley, and D. P. Shelton, J. Chem. Phys. **108**, 849 (1998)

[12] V. Mizrahi and D. P. Shelton, Phys. Rev. A, **31**, 3145. (1985)

[13] C. K. Miller and J. F. Ward, Phys. Rev. A, **16**, 1179 (1977)

[14] D. P. Shelton and A. D. Buckingham, Phys. Rev. A, **26**, 2787 (1982)

[15] D. P. Shelton, Phys. Rev. A **42**, 2578 (1990)

[16] K. Ohta, et. al., Mol. Phys. **101**, 315 (2003)

VITA

Graduate College
University of Nevada, Las Vegas

Scott Wilde

Degrees:
Bachelor of Science, Physics, 2008
University of Nevada, Las Vegas

Thesis Title: Dispersion of the Hyperpolarizability of the Carbon Tetrachloride Molecule

Thesis Examination Committee:
Chairperson, Dr. David P. Shelton, Ph. D.
Committee Member, Dr. Victor H. S. Kwong, Ph. D.
Committee Member, Dr. Stephen Lepp, Ph. D.
Graduate Faculty Representative, Dr. Chulsung Bae, Ph. D.